



COMPARISON BETWEEN EFFECTS OF BODY AND SURFACE WAVES ON TORSIONALLY COUPLED SOIL-STRUCTURE SYSTEMS

FARHAD BEHNAMFAR and SATOSHI KURITA

Department of Architecture and Building Engineering , Tohoku University
Sendai 980-77, Japan

ABSTRACT

It is common in practice of building design to suppose a ground motion consisting only of vertically incident shear waves. Such an idea neglects the spatial variation of ground motion under the base of the building . In this study effects of incoherent ground motion on earthquake response of torsionally asymmetric buildings resting on flexible soil are investigated and various types of waves are considered.

KEYWORDS

earthquake response, incoherent ground motion, asymmetric buildings, soil-structure interaction, body and surface waves.

INTRODUCTION

In practical seismic design of conventional buildings it is common that ground motion to be taken as constant over all points of structure-soil interface and structure is assumed to have a fix base. Although for a structure based on bedrock that is a reasonable assumption, but it is not the case for flexibly supported buildings. Presence of building affects the free-field motion of a flexible site considerably and the total dynamic system consisting of soil and structure is completely different than the rigid-soil assumption. To solve the problem, usually effective input motion taking account for spatial variation of excitation is calculated either by averaging the varying ground motion over surface of foundation (Iguchi, 1982; Hahn and Liu, 1994) or discretizing the structure-soil interface into elements and using boundary element method (Wolf, 1985). Then a dynamic model for soil-structure system is constructed which includes the desired dynamical characteristics of the soil and the structure.

In this study, a one story model of a general unsymmetric multistory building resting on flexible soil is selected. Using elastic theory of wave propagation, various body and surface waves representing the ground excitation are formulated. Then a parametric study revealing important features of dynamic behavior of the system is done. The main purpose is to evaluate the lateral and torsional response of the system with different degrees of asymmetry under different types of waves.

DYNAMIC MODEL

Figure 1 shows the dynamic model used in this study. It consists of a one-story building with mass m and height h which models a general unsymmetric multi-story building, a rigid-circular foundation with the

mass m_0 and radius r , and a flexible half-space with hysteretic damping ratio ξ_g , Poisson ratio ν and shear wave velocity v_s .

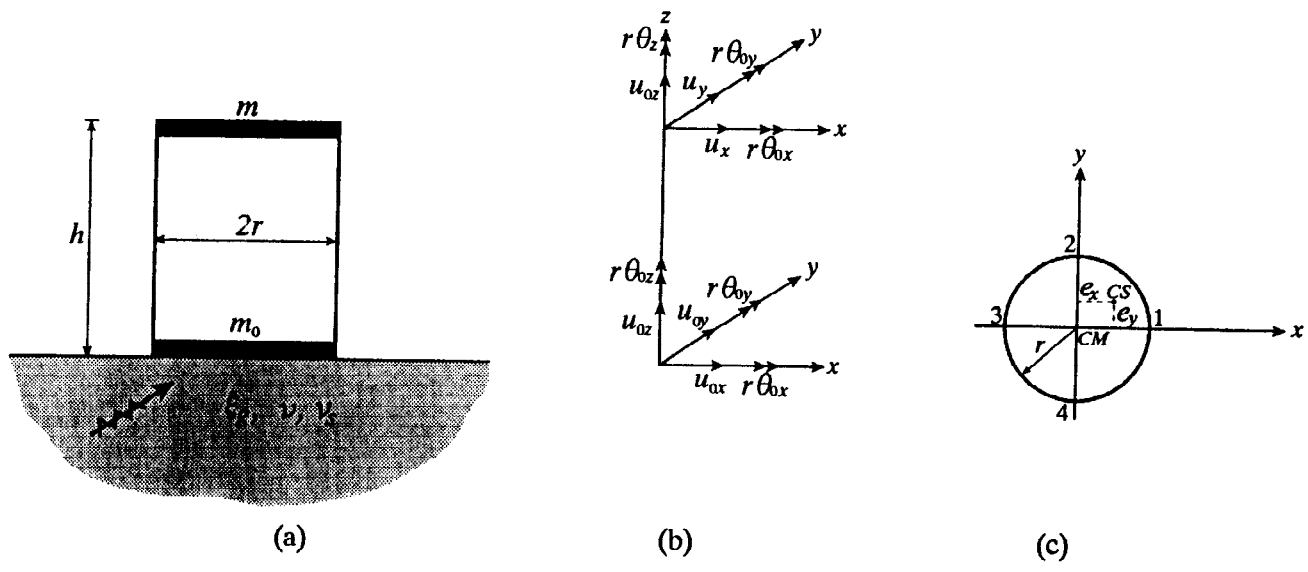


Fig. 1. a) dynamic model; b) degrees of freedom; c) plan of story (mass m).

The system is defined with the following dimensionless parameters:

- 1) Non-dimensional frequency $\bar{\omega} = \omega r/v_s$ in which ω is frequency of excitation, r is radius of circular plan of building's story as well as foundation, v_s is shear wave velocity in underlying soil.
- 2) Dimensionless height $\bar{h} = h/r$.
- 3) Mass ratio $\bar{m} = m_0 / (\rho r^3)$ in which ρ is mass density of the elastic half-space.
- 4) The stiffness ratio of the system in lateral motion $\bar{\omega}_l = \omega_l h/v_s$ in which ω_l is fixed-base frequency of the structure in lateral motion. It may be different for x and y directions.
- 5) The stiffness ratio of the system in torsional motion $\bar{\omega}_t = \omega_t h/v_s$ in which ω_t is fixed-base torsional frequency of the structure.
- 6) Ratio of eccentricity in x -direction $\bar{e}_x = e_x/r$ and in y -direction $\bar{e}_y = e_y/r$; in which e_x and e_y are stiffness eccentricities of the plan of the building along the x and y directions, respectively. Corresponding to positive values of \bar{e}_x and \bar{e}_y , points 1 and 2 of the plan of building in figure 1c show the stiff sides of the building.
- 7) Hysteretic damping ratio of building ξ .

In this study the following numerical values are used: $\bar{h} = 1.0$ and $\bar{\omega}_x = \bar{\omega}_y = \bar{\omega}_t = 2.0$ which are associated with relatively stiff buildings for them soil-structure interaction is more highlighted, $m_0/m = 0.33$, $\xi = 0.07$, $\xi_g = 0.05$ and $\nu = 0.33$.

Nine degrees of freedom is used for the system: two horizontal and one torsional motion for the mass m and all the six possible degrees of freedom for the mass m_0 .

METHOD OF ANALYSIS

Dynamic equations of motion in frequency domain are written and summarized in matrix form as is shown in equation 1:

$$[S]\{U\} = \{P\} \tag{1}$$

In the above equation, $\{U\}$ is the 9×1 vector of unknown responses, $\{P\}$ is the 9×1 load vector consisting of appropriate combinations of input motion of the foundation having 6 degrees of freedom: displacements

along x, y, and z axes and rotations about the same axes. Input motion of a surface foundation which is equal to its kinematic response (Wolf, 1985), is calculated from the free-field earthquake motion. It has been known that this "effective motion" is highly related to the ratio r/v_a in which v_a is the apparent wave velocity in the horizontal direction which is equal to $v_s/\cos\alpha$ for body waves whereby α is angle of incidence of S- or P-wave measured from the horizontal. For surface R-waves, again v_a is a function of ξ_g, ν , and v_s . For undamped soils and $\nu = 0.33$, v_a for Rayleigh waves (R-waves) is $0.933 v_s$. $[S]$ is 9×9 dynamic stiffness matrix of system consisting stiffness terms of structure and soil. $[S]$ is calculated using the dimensionless parameters as above and stiffness and damping of soil. The value of these latter terms are calculated by discretizing the soil-structure interface into elements and making use of the conventional boundary element method (Wolf, 1985). The same method is used for calculating the effective input motion from the free-field earthquake excitation. Seismic motion is supposed to be consisted of body SH, SV, and P waves, and surface Rayleigh waves propagating along x-axis, but each time only one type of the waves is included in the input motion.

DYNAMIC ANALYSIS AND RESULTS

Figure 2 shows the result of the analysis of system for harmonic loading of an SH-wave. It is clearly visible that while horizontal response of system for horizontal incidence decreases by about 10 percent comparing to vertical incidence, a strong torsional response arises. Figure 3 shows the phase angle between lateral and torsional displacements. It is seen that for most of the frequency domain (except for $\bar{\omega} < 1$), the motion is 180° out of phase resulting considerable difference between displacements of stiff and soft sides of building (points 1 and 3 in figure 1c, respectively). In figure 4 ratio of lateral displacements of these corner points is depicted that shows strong values at two torsional-mode frequencies of the system. Also, for high frequencies this ratio is highly related to the degree of eccentricity. In figures 5, 8 and 10 lateral and torsional motions of system for propagating SV-, P- and R-waves are shown. The selected incident angles of SV- and P- waves are associated with highest responses. Strong torsional response is seen for $c/r > 0.3$ while effect of the Rayleigh waves is considerably higher. The same behavior is observed in figures 6, 7, 9, 11, and, 12. Also, in figure 9 higher torsional response is seen for lower mass ratios \bar{m} , i.e., for lighter foundations or the ones with greater areas.

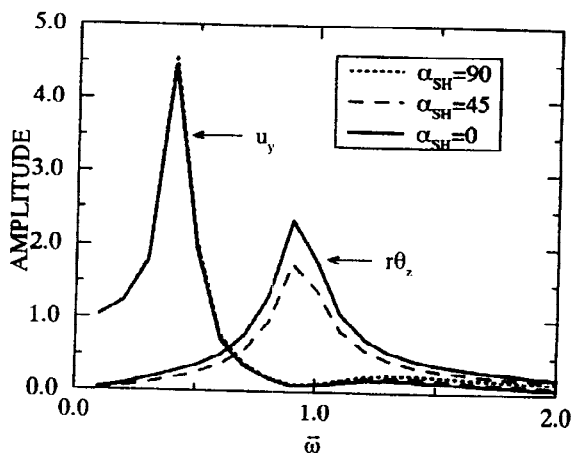


Fig. 2. Spectra of u_y and $r\theta_z$, SH-wave as harmonic, $\bar{m} = 2.25$, $\bar{e}_x = 0$.

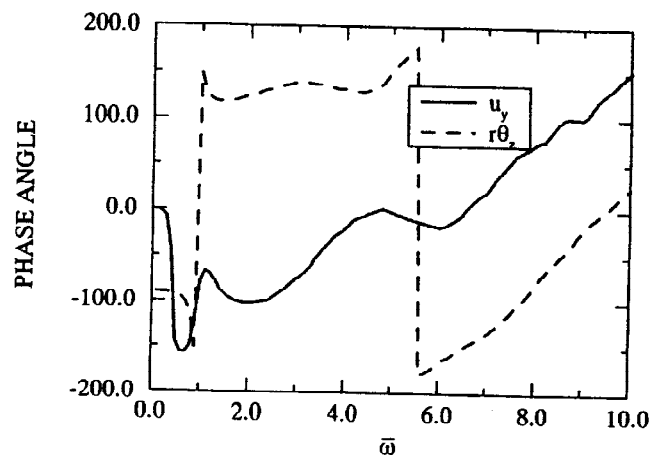


Fig. 3. Phase angles of u_y and $r\theta_z$, SH-wave as harmonic, $\bar{m} = 2.25$, $\bar{e}_x = 0$, $\alpha_{SH} = 0$.

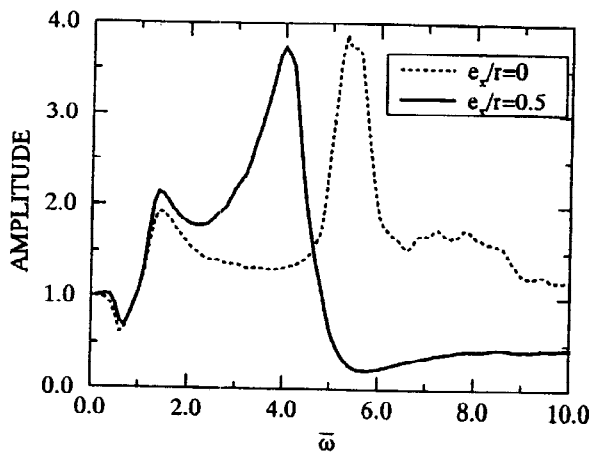


Fig. 4. Spectrum of ratio $|u_{y3}/u_{y1}|$, SH-wave as harmonic, $\bar{m}=2.25, \alpha_{SH}=0$.

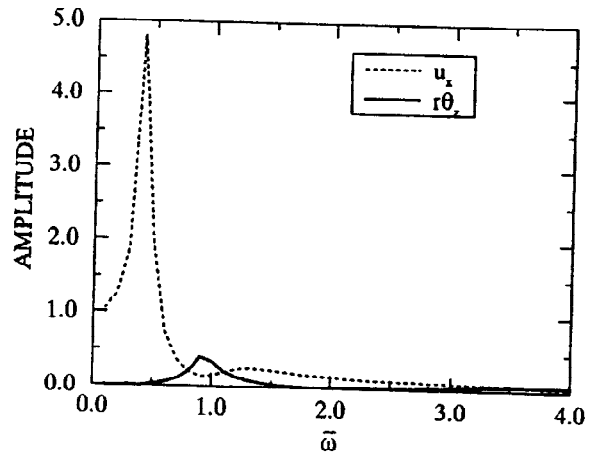


Fig. 5. Spectra of u_x and $r\theta_z$, SV-wave as harmonic, $\bar{m}=2.25, \bar{e}_y=0.5$.

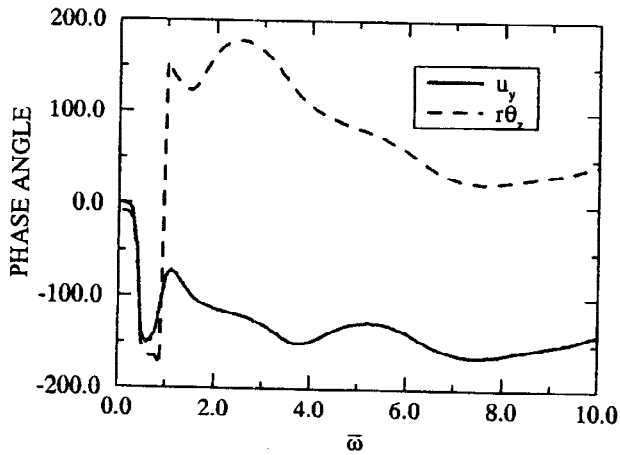


Fig. 6. Phase angles of u_x and $r\theta_z$, SV-wave as harmonic, $\bar{m}=2.25, \bar{e}_y=0.5$.

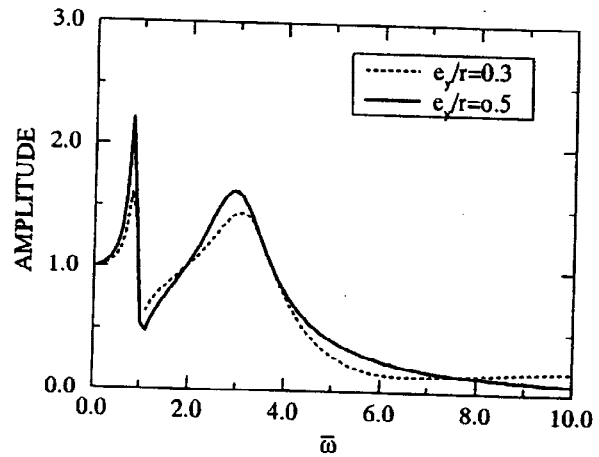


Fig. 7. Spectrum of ratio $|u_{x4}/u_{x2}|$, SV-wave as harmonic, $\bar{m}=2.25, \alpha_{SV}=70$.

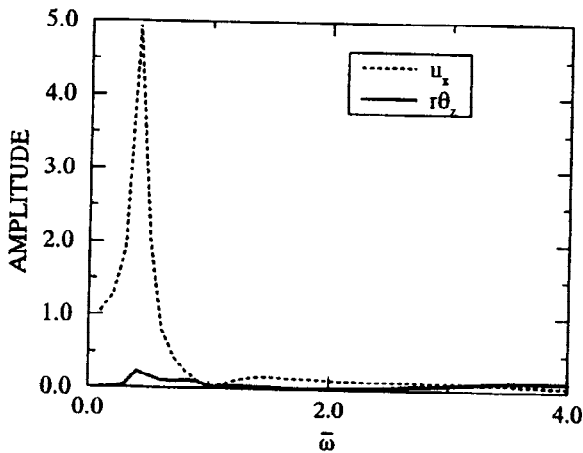


Fig. 8. Spectra of u_x and $r\theta_z$, P-wave as harmonic, $\bar{m}=2.25, \bar{e}_y=0.5, \alpha_P=55$.

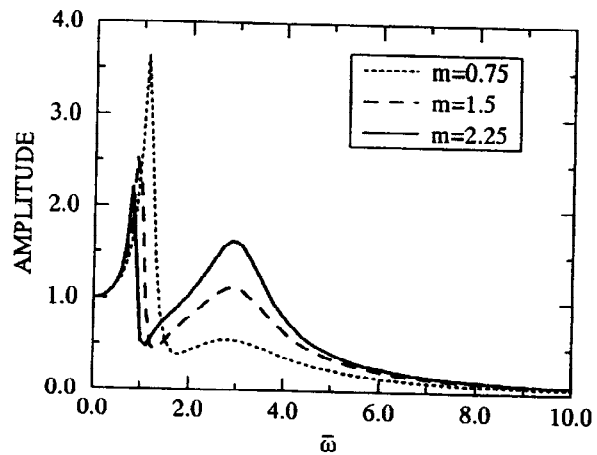


Fig. 9. Spectrum of ratio $|u_{x4}/u_{x2}|$, P-wave as harmonic, $\alpha_P=55, \bar{e}_y=0.5$.

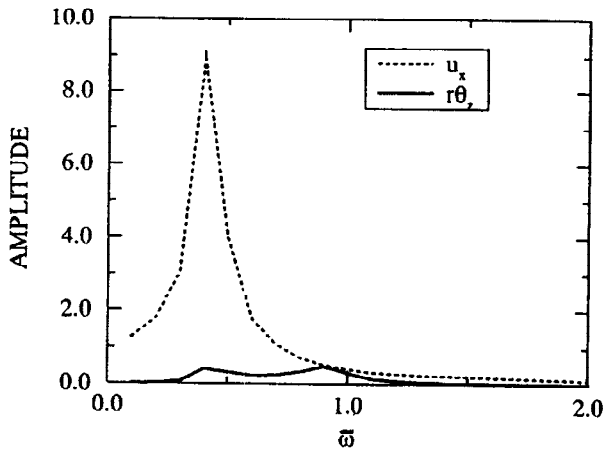


Fig. 10. Spectra of u_x and $r\theta_z$, R-wave as harmonic, $\bar{m}=2.25$, $\bar{e}_y=0.5$.

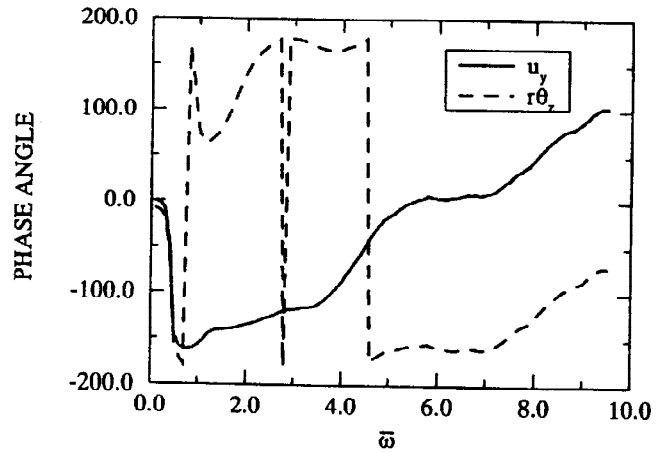


Fig. 11. Phase angles of u_x and $r\theta_z$, R-wave as harmonic, $\bar{m}=2.25$, $\bar{e}_y=0.5$.

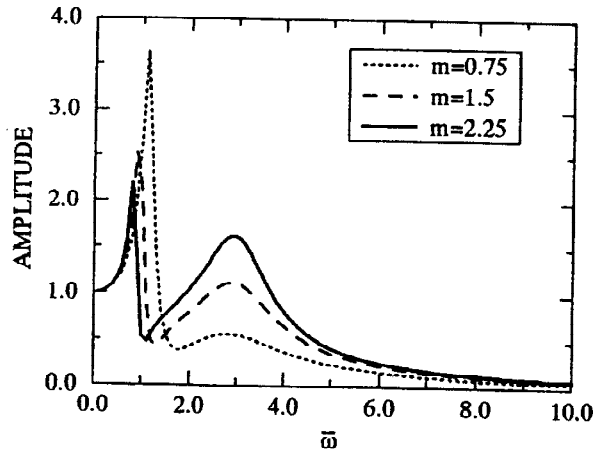


Fig. 12. Spectrum of ratio $|u_{x4}/u_{x2}|$, R-wave as harmonic, $\bar{e}_y=0.5$.

The same system is analyzed for the N-S component of El-Centro 1940 earthquake. Figure 13 is an in-structure acceleration response spectrum of the stiff and soft sides (points 1 and 3 in figure 1c) which shows an additional strong peak at fundamental torsional frequency of system. Also in this figure considerable differences between response of corner points 1 and 3 for $f > 2$ Hz is seen. Figure 14 shows the variation of lateral acceleration response of structure due to incident R-waves normalized to those of SV- and P-waves. This again shows the higher effect of R-waves for lower frequencies. Finally in figure 15 the ratio of responses of corner points 2 and 4 (figure 1c) for incident R-waves is shown. The difference is higher for larger frequencies.

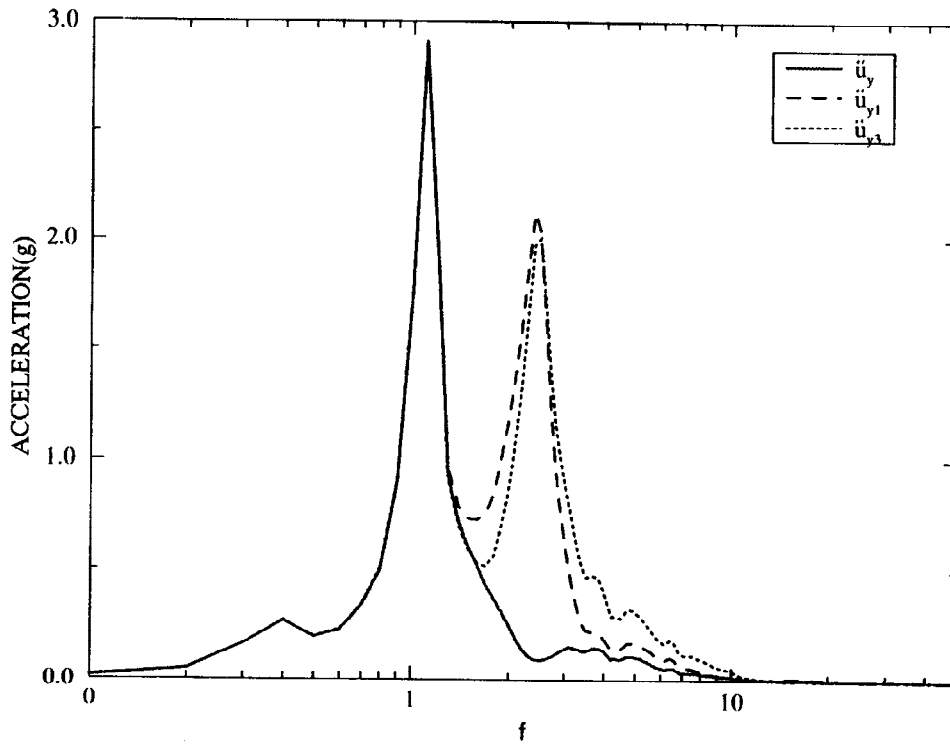


Fig. 13. Acceleration response spectra, N-S component of El-Centro 1940 as free-field motion associated with SH-wave, $\alpha_{SH} = 0.0^\circ$, $\bar{m} = 2.25$, $\bar{e}_x = 0.5$, $r/v_s = 0.06s$.

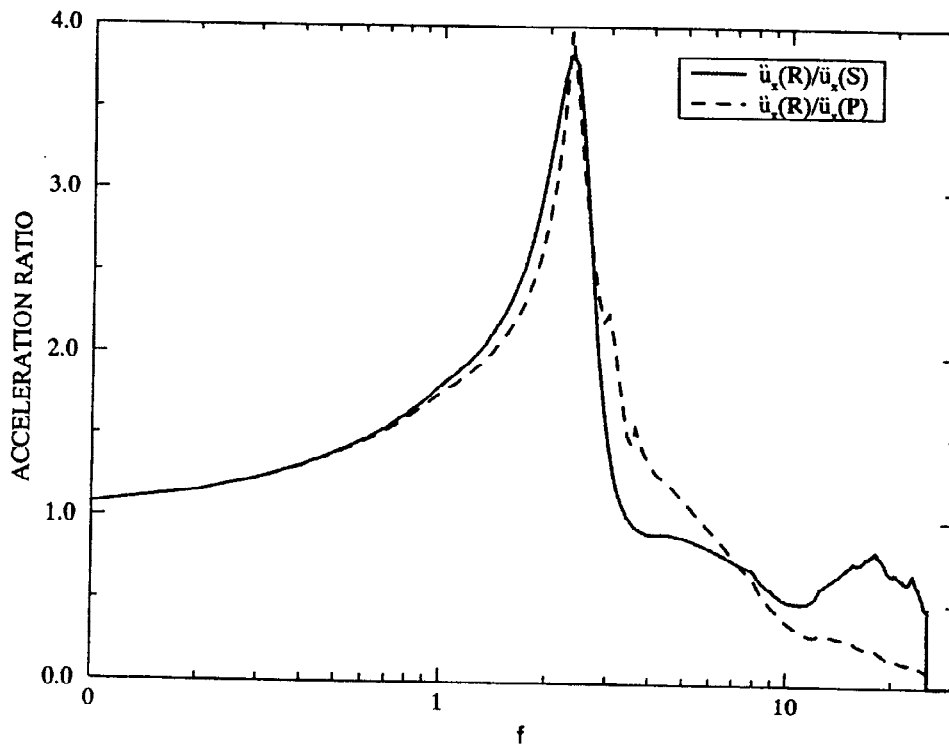


Fig. 14. Acceleration response spectra of \ddot{u}_x for R-waves normalized to those of SV- and P-waves, N-S component of El-Centro 1940 as free-field motion associated with R-, SV-, and, P-waves, respectively; $\alpha_{sv} = 70^\circ$, $\alpha_p = 55^\circ$, $\bar{m} = 2.25$, $\bar{e}_y = 0.0$, $r/v_s = 0.06s$.

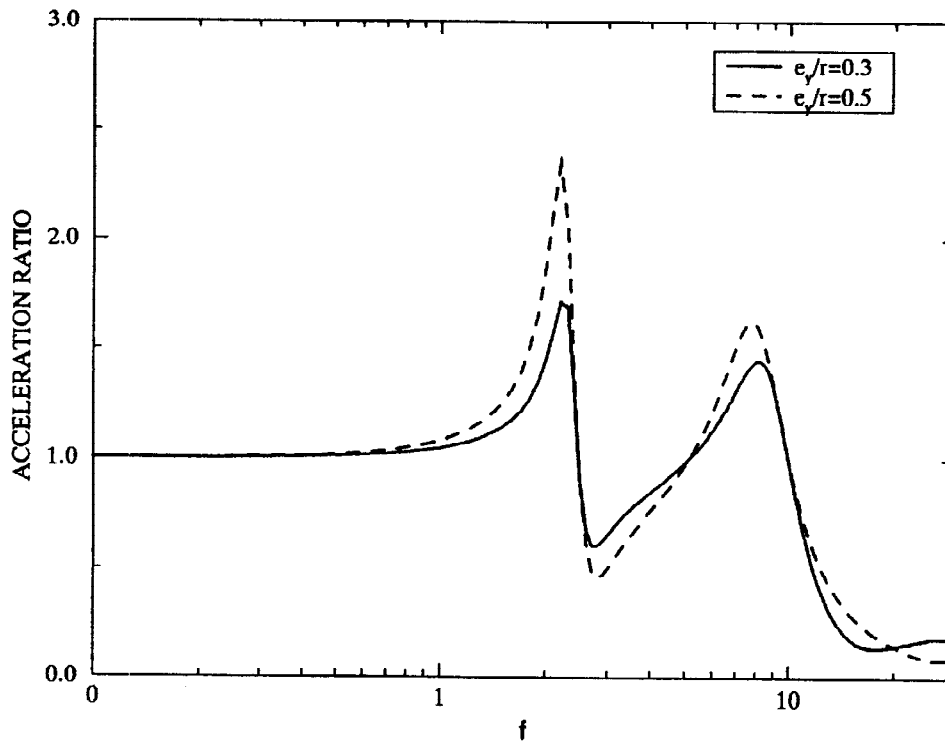


Fig. 15. Acceleration spectrum of $\ddot{u}_{x4}/\ddot{u}_{x2}$, N-S component of El-Centro 1940 as free-field motion associated with R-waves, $\bar{m}=2.25$, $r/v_s=0.06s$.

CONCLUSION

Based on the results of this study, it can be concluded that:

1. Horizontally propagating waves have remarkable increasing effects on response of unsymmetric soil-structure systems.
2. For shallow incidence of SH waves, a big torsional input motion is induced to the structure that gives rise to the torsional response of system due to unsymmetry.
3. In the case of SV, P and R waves, torsional response is increased for buildings having foundations with lower masses or to a much higher degree, with larger areas (greater radius).
4. Response of higher levels of building is much more sensitive to R waves than other types of waves.

ACKNOWLEDGEMENT

The first author expresses his gratitude to the ministry of culture and higher education of Iran for financial support during this study.

REFERENCES

- Hahn G. D. and Liu X. (1994). Torsional Response of Unsymmetric Buildings To Incoherent Ground Motion. *Journal of Structural Engineering, ASCE*, **120**, No. 4, 1158-1181.
- Iguchi, M., (1982). An Approximate Analysis of Input Motions for Rigid Embedded Foundations. *Transactions of Architectural Institute of Japan*, **315**, 61-73.
- Sikaroudi H. and Chandler A. M. (1992). Structure-Foundation Interaction in the Earthquake Response of Torsionally Asymmetric Buildings. *Soil Dynamics and Earthquake Engineering*, **11**, 1-16.
- Wolf, J. P., (1985). *Dynamic Soil-Structure Interaction*. Prentice-Hall, Inc.